INSTITUTE OF PHYSICS PUBLISHING PLASMA PHYSICS AND CONTROLLED FUSION

Plasma Phys. Control. Fusion **44** (2002) B159–B172 PII: S0741-3335(02)53216-4

MHD spectroscopy

A Fasoli[1,2], D Testa[2], S Sharapov[3], H L Berk[4], B Breizman[4], A Gondhalekar[3], R F Heeter[5], M Mantsinen[3] and contributors to the EFDA-JET Workprogramme[6]

[1] CRPP-EPFL, Association EURATOM-Confédération Suisse, 1015 Lausanne, Switzerland
[2] Plasma Science and Fusion Center, MIT, Cambridge, MA 02139, USA
[3] EURATOM-UKAEA Fusion Association, Culham Science Center, Abingdon, UK
[4] Institute for Fusion Studies, University of Texas at Austin, Texas 78712, USA
[5] Lawrence Livermore National Laboratory, CA 94550, USA

Received 10 September 2002
Published 21 November 2002
Online at stacks.iop.org/PPCF/44/B159

Abstract

Experiments are conducted on the JET tokamak to demonstrate the diagnostic potential of Magneto-Hydro-Dynamics (MHD) spectroscopy, for the plasma bulk and its suprathermal components, using Alfvén eigenmodes (AEs) excited by external antennas and by energetic particles. The measurements of AE frequencies and mode numbers give information on the bulk plasma. Improved equilibrium reconstruction, in particular in terms of radial profiles of density and safety factor, is possible from the comparison between the antenna driven spectrum and that calculated theoretically. Details of the time evolution of the non-monotonic safety factor profile in advanced scenarios are reconstructed from the frequency behaviour of ICRH-driven energetic particle modes. The plasma effective mass is inferred from the resonant frequency of externally driven AEs in discharges with similar equilibrium profiles. The stability thresholds and the nonlinear development of the instabilities give clues on energy and spatial distribution of the fast particle population. The presence of unstable AEs provides lower limits in the energy of ICRH generated fast ion tails. Fast ion pressure gradients and their evolution are inferred from the stability of AEs at different plasma radial positions. Finally, the details of the AE spectrum in the nonlinear stage are used to obtain information about the fast particle velocity space diffusion.

1. Introduction

Collective modes are a special property of the plasma state. In fusion research, they are commonly studied for two reasons. First, to assess and limit their negative effect on the

[6] See appendix of Pamela J *et al* 2001 *Proc. 18th International Conf. on Fusion Energy 2000 (Sorrento, 2000)* (Vienna: IAEA).

plasma performance, in particular on the confinement and transport of energy and particles. Conditions in which the modes are either stable or can be kept at amplitudes that are too low to affect the plasma behaviour are sought. Second, to find ways to couple energy via electromagnetic waves from external antennas in order to heat the plasma. Here we discuss a third aim for investigating the properties of collective plasma modes in fusion devices, namely on how to extract information on the plasma. Because of the low frequency range of the modes that are used for diagnostic purposes, this approach is referred to as Magneto-Hydro-Dynamics (MHD) spectroscopy [1].

To serve diagnostic purposes for the plasma bulk as well as for suprathermal components of the plasma, the collective modes must satisfy a number of requirements. Their dispersion relation should depend on the macroscopic properties of the plasma, separate from the instability drive, which should come from non-thermal components or fast particles. The modes should not be subject to strong damping, with their phase velocity well separated from both the ion and electron thermal speeds, and should exist in a frequency range that is naturally free of significant background turbulence. It should be possible to drive and detect the modes at amplitudes that are low enough to avoid significant perturbations to the plasma equilibrium and transport. The above requirements are satisfied by modes in the Alfvén wave range of frequencies.

In toroidal plasmas, the dispersion relation for Alfvén waves is locally satisfied point by point along the radial profile, giving rise to the so-called Alfvén continuum, described by $f_{\mathrm{A}}(r) = k_{||}(r)v_{\mathrm{A}}(r)/2\pi$, which in cylindrical approximation reads

$$f_{\mathrm{A}}(r) = \frac{v_{\mathrm{A}}}{2\pi R}\left(n + \frac{m}{q(r)}\right), \qquad v_{\mathrm{A}} = \frac{B}{\sqrt{4\pi n_i m_i}} \tag{1}$$

Here v_{A} is the Alfvén speed, n and m the toroidal and poloidal mode numbers, R the torus major radius, and $q(r)$ the safety factor profile. Due to the continuous dependence of the frequency on position, continuum modes are strongly damped. The coupling of different poloidal harmonics produces gaps within which weakly damped Alfvén eigenmodes (AEs) exist [2], such as Toroidal AEs, in the gap centred at $f_{\mathrm{TAE}} = v_{\mathrm{A}}/(4\pi q R)$, and Elliptical AEs, with $f_{\mathrm{EAE}} \sim 2f_{\mathrm{TAE}}$. The drive for these modes stems from the free energy source associated with the radial pressure gradient of particles with energies such that their velocities are of the order of the Alfvén speed. For passing particles the resonance condition is expressed in terms of the velocity parallel to the magnetic field, $v_{||} \sim v_{\mathrm{A}}$ for the primary resonance and $v_{||} \sim v_{\mathrm{A}}/3$, $v_{\mathrm{A}}/5$, and so on for higher order resonances, of decreasing significance. For trapped particles, the resonance occurs between the wave and the bounce or precession motions, corresponding to particle velocities $|v| = v_{\mathrm{A}}/2(R/r)^{1/2}$ and $|v| = v_{\mathrm{A}}/2qk_\theta\rho_{\mathrm{L}}$, respectively [3].

In JET different sources for non-thermal ions exist, including neutral beam injection (NBI) and fusion reactions generating 3.5 MeV α's in deuterium–tritium (D–T) plasmas. However, in this paper we will focus on fast ions generated by ion cyclotron resonance heating (ICRH). The most commonly used scheme is hydrogen minority heating in deuterium plasmas, in which the H^+ ions typically resonate with Alfvén waves for ion energies of the order of 0.5 MeV.

The resonance condition is a necessary but not sufficient condition to drive AEs unstable. A strong fast particle pressure gradient is necessary to overcome the Landau damping due to the fast particles themselves and the damping coming from the background plasma. The drive from the fast particles leads to a growth rate of the AE instability that can be expressed as

$$\gamma = \int \left[\omega\frac{\mathrm{d}F}{\mathrm{d}E} - \text{const.} \times n\frac{\mathrm{d}F}{\mathrm{d}r}\right] F_{\text{resonance}}(v, v_{\mathrm{A}})\,\mathrm{d}v \tag{2}$$

where F is the fast particle distribution function, E the particle energy, and $F_{\text{resonance}}(v, v_{\mathrm{A}})$ expresses the resonance condition discussed above.

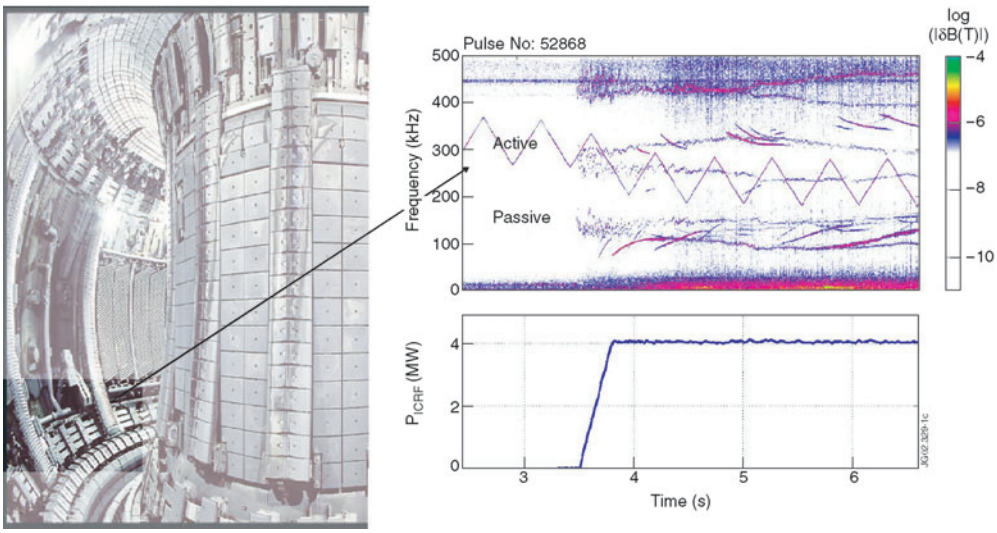

Figure 1. Example of co-existence of active and passive MHD spectroscopy. Here and in the following figures the plasma is started at $t = 0$ s.

Figure 1 (right) presents a characteristic AE spectrum in a JET discharge with about 4 MW of ICRH additional heating in the H-minority heating scheme. As expected, TAEs and EAEs appear in a turbulence free zone of the spectrum in the corresponding gaps of the Alfvén continuum. Their amplitude, $\delta B/B \sim 10^{-6}$ as measured at the plasma edge, does not seem to produce any significant effect in the plasma, nor to affect the ICRH power deposition process significantly. Each mode measured in the laboratory frame is subject to Doppler shift due to the plasma rotation, with $\mathrm{f}_{\mathrm{meas}} = f_{\mathrm{AE}} + n f^{\mathrm{tor}}_{\mathrm{rot}}(r_{\mathrm{AE}})\ [+m f^{\mathrm{pol}}_{\mathrm{rot}}(r_{\mathrm{AE}})]$. Here r_{AE} is the position of the eigenmode. The term with the poloidal rotation appearing in brackets is neglected as is usually small in comparison with the toroidal rotation term.

We will discuss the experimental methods to investigate the AE properties, passive and active MHD spectroscopy, in section 2. Section 3 is dedicated to the extraction of information on the plasma bulk, namely on the plasma equilibrium density and safety factor profiles, and on the plasma effective mass, from the measurement of the mode frequency. Section 4 explores the possibility of inferring properties of the suprathermal ion distribution, both in real and in configuration spaces, from the mode stability limits and from the nonlinear evolution of unstable modes. A summary of the results and an outlook for future experiments are included in the section 5.

2. Experimental method

Two experimental methods, passive and active MHD spectroscopy, are used at JET to obtain information on the plasma and its non-thermal components.

2.1. Passive MHD spectroscopy

Passive MHD spectroscopy simply consists in observing collective modes in the Alfvén frequency range driven unstable by fast particles using edge and internal fluctuation measurements. Magnetic probes measuring $\mathrm{d}\delta B_{\mathrm{pol}}/\mathrm{d}t$ at the plasma edge provide the clearest

signals. For simplicity, only spectral data from this system will be used throughout this paper. The fluctuation signals are digitized for 4 s at 1 MHz, with 12 bits resolution, by the 8-channel KC1F system. The distribution of the probes connected to KC1F allows us to reconstruct toroidal mode numbers in the range from $n = -17$ to +17 and to measure local poloidal phases. All magnetic probe channels are calibrated remotely; the calibration is implemented as a digital filter applied to the raw data [4]. Unstable modes with amplitudes as low as $|\delta B| \sim 10^{-8}$ T can be detected.

2.2. Active MHD spectroscopy

Active MHD spectroscopy refers to the technique of driving low amplitude perturbations in the plasma using external antennas, and extracting the plasma response using synchronous detection. At JET, signals from magnetic coils, electron cyclotron emission (ECE), reflectometer and x-ray cameras are employed. Different combinations of antenna phasing for 1, 2 or 4 saddle coils can be chosen to excite specific low toroidal mode numbers ($n = 0, 1, 2$). Maximum current and voltage are of the order of 30 A and 1000 V, corresponding to core magnetic perturbations ($\delta B/B < 10^{-5}$) too weak to produce significant effects on the bulk plasma or on the fast particle confinement.

The plasma collective modes appear as resonances in the measured plasma response. Their frequency, mode structure and background damping rate can therefore be measured in the absence of resonant fast particles. When resonant particles are present, but the instability drive is insufficient to drive the modes unstable, active spectroscopy still provides estimates of fast particle drive and background plasma damping separately [5].

Figure 1 (left) highlights one of the four saddle coils presently installed inside the JET vacuum vessel. The spectrogram of a magnetic probe at the plasma edge shown in figure 1 (right) illustrates both active and passive spectroscopic methods in action in a plasma discharge. The trace labelled 'active' corresponds to the magnetic perturbation driven in the plasma by the saddle coils, and is well visible on the spectrogram before any fast particles are present. Once the ICRH power exceeds the threshold for driving AEs unstable, the magnetic signals corresponding to ICRH-driven TAEs and EAEs are visible and coexist with the active signal.

When time resolved measurements of properties of the driven mode are needed, a digital real time control system is used to perform individual resonance tracking. The controller of the exciter frequency, run at a 1 ms clock rate, varies the frequency linearly around the initial guess for the AE resonance, generally at the centre of the AE gap. When the AE resonance is met, the exciter frequency is swept back and forth around it. The time taken to cross each resonance, typically of the order of 30 ms, represents the typical time resolution of the measurement of frequencies and damping rates. As the simple estimate of frequency and damping rate from the centre and width of the driven resonance follows closely the value obtained from a full fit [6], these quantities can be evaluated in real time. Figure 2 illustrates an example of tracking an individual collective mode in a plasma in the absence of AE instability drive. On the right, the magnitude of the synchronously detected magnetic probe signal is plotted as a function of frequency and time. The signal peaks when the frequency of the exciter crosses the calculated centre of TAE gap, f_{TAE}, allowing an unambiguous identification of the driven modes as $n = 1$ TAEs. The detail shows a single peak corresponding to an $n = 1$ TAE resonance crossing. The magnetic spectrogram on the left for the time interval 53–57 s confirms that the antenna driven perturbation completely dominates the fluctuation spectrum in the AE frequency range.

The low toroidal mode numbers that can be driven by the JET saddle coils are strongly damped in plasmas of high elongation and edge magnetic shear, hence becoming undetectable during the divertor phase of the discharge [7]. Although this finding represents a positive

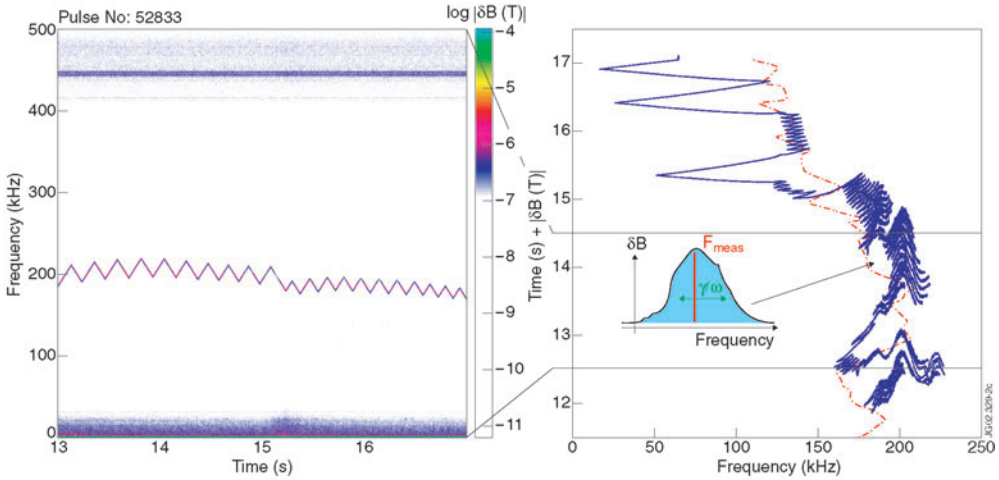

Figure 2. Tracking of an individual AE (an $n = 1$ TAE) in the absence of fast particle drive in the limiter phase of a JET ohmic discharge, with the synchronously detected signal (right), and the spectrogram of the directly digitized magnetic perturbation (left).

piece of news for future burning plasma experiments, in most cases it prevents the use of MHD spectroscopy in the high performance phase of the JET discharges. In addition, intermediate or high toroidal mode numbers characterize the most unstable AEs detected in JET and predicted for ITER. A direct excitation and tracking of the same modes would therefore be of interest for preparing the next step experiments.

To overcome these limitations, a structure optimized for the excitation and detection of AEs with $n \leqslant 15$ is being designed for future applications in JET. Eight antennas in two groups of four are foreseen. Each antenna is made of 7-turns of conductor, of a size of about 20 cm $\times$ 20 cm $\times$ 15 cm, separated from each other by about 15 cm, and is characterized by a static self-inductance for each antenna of the order of $L \sim 15\,\mu$H. The distance between the antennas and the last closed flux surface is the order of 10 cm. A sketch of the proposed design is shown in figure 3. Four of the eight antennas will be driven at the same time, chosen to obtain the specific toroidal mode number spectrum needed for a given experiment. The un-energized antennas will be used as detectors.

3. From the wave frequency to plasma bulk properties

The measurement of the mode frequency performed in the laboratory frame is subject to Doppler shift due to plasma rotation, which can be significant in the presence of NBI additional heating. By measuring the Doppler shift in the frequency of the ICRH-driven AEs with different n, the value of the plasma rotation velocity at the mode location is inferred. Such measurements indicate that a significant difference in the rotation of the bulk and impurity ions exists in the presence of strong pressure gradients [8].

As shown in equation (1), the dispersion relation of Alfvén waves in a torus depends on the safety factor profile $q(r)$, and the plasma effective mass, in addition to the magnetic field and density. In the following we will show examples of information obtained on $q(r)$ from active and passive spectroscopy, and on the plasma isotopic mix from active mode tracking in D–T plasmas.

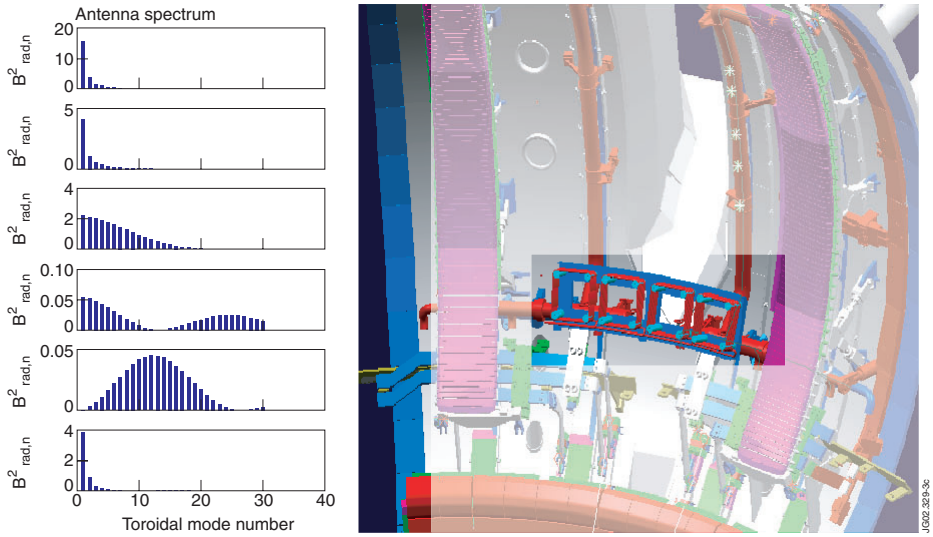

Figure 3. A sketch of four of the eight new AE antennas designed for JET-EP, along with the expected geometrical toroidal mode number spectrum for a number of possible phase combinations, for the radial component of the magnetic field. A second block of four antennas will be installed diametrically opposed in the vacuum vessel.

3.1. Static q-profile from active MHD spectroscopy: improvement of equilibrium reconstruction

In addition to weakly damped eigenmodes in the gap, external antennas can drive the Alfvén continuum and measure the structure of the corresponding plasma response. As the structure of the Alfvén continuum in a tokamak depends on $q(r)$ and the density profile, $n_e(r)$, information on these can be gathered. Relatively cold JET ohmic plasmas, in the limiter phase of the discharge, are considered, as in this case kinetic effects such as the creation of multiple AEs at the top of the relevant gap are not observed to play an important role [9]. The experimental curve is compared to the results of a numerical calculation based on the fluid model CASTOR [10]. In order for the two curves to match, the standard equilibrium reconstruction has to be modified, namely the central part of the safety factor profile and the edge portion of the density profile [11].

When more than one core localized TAE exist for a given mode number, the frequency separation of the modes is related to the width of the Alfvén gap in the core. As this depends on the value of q at the plasma centre, as shown in figure 4 (left), the comparison of the measured antenna driven spectrum with that calculated from fluid theory leads to a good estimate of the value of $q(0)$. This is demonstrated in figure 4 (right), which shows on the same frequency axis the calculated and measured mode spectrum in terms of the antenna loading, i.e. the power absorbed in the plasma per period of the driving frequency, and of the magnitude of the magnetic perturbation at the plasma edge, respectively.

The accuracy of this method can be rather good, up to $\pm 10\%$ for $q(0)$, but it depends critically on the quality of the initial guess for the equilibrium and requires a laborious comparison between the data and the results of numerical codes. As the frequency range that the antenna has to cover to measure the continuum plasma response and/or several modes in the gap is rather large, the intrinsic time resolution is limited to no less than 100–200 ms.

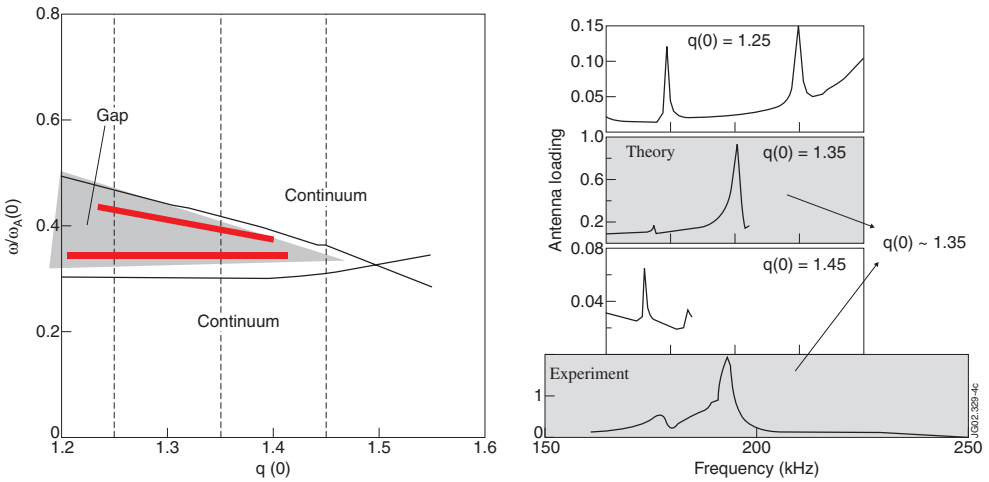

Figure 4. Comparison of data and fluid theory results on the antenna loading for a case in which two core-localized $n = 1$ TAEs are present on the gap [11]. The dependence of the gap width and mode frequency on $q(0)$ is shown on the left, while the adjustment of $q(0)$ to obtain a good fit of the data appears on the right; the calculated and measured spectrum is plotted on the same frequency axis in terms of the antenna loading, i.e. the power absorbed in the plasma per period of the driving frequency, and of the amplitude of the magnetic perturbation at the plasma edge, respectively.

3.2. Dynamic q-profile: determination of $q_{\min}$ from Alfvén Cascades

In advanced scenarios it is important to obtain information on the time evolution of the safety factor profile. Details of $q(r, t)$ are in fact related to the creation of regions in the plasma core within which the turbulence-induced transport can be significantly reduced, improving the plasma performance [12]. Passive MHD spectroscopy on modes that are excited by ICRH can be used to this purpose.

The experimental observations indicate that in the presence of a non-monotonic q-profile, generated by lower hybrid current drive in the pre-heating phase of the discharge, a new class of Alfvén waves is driven by ICRH [13, 14]. As their existence, in addition to their drive, is associated with supra-thermal ion populations, these modes belong to the general class of energetic particle modes (EPM) [15, 16]; owing to their fast frequency sweep in time, those observed in the JET reversed shear discharges are named Alfvén cascades (ACs) [16].

Each cascade consists of several modes with different toroidal mode numbers, typically from $n = 1$ to 6. The different frequencies are subject to upward sweeping, starting from 20 to 60 kHz, below the TAE gap, and increasing up to the frequency of the TAE gap. The rate of increase in the frequency is proportional to the mode number, as apparent from figure 5 (right), where a typical sequence of cascades is shown in terms of the measured toroidal mode numbers as a function of frequency and time.

The AC frequency sweeping shows a very close correlation with the time evolution of the local extremum, or *tip* of the Alfvén continuum, where $\mathrm{d}f_{\mathrm{A}}/\mathrm{d}r = 0$, which in turn is associated with the minimum of the q-profile, $q_{\min}$. This suggests that the observations correspond to a new type of EPMs found theoretically just above the *tip* of continuum, localized at the radial position of $q_{\min}$, with an eigenfrequency given by [17]

$$f_{\mathrm{AC}}(t) \approx \left| \frac{m}{q_{\min}(t)} - n \right| \frac{v_{\mathrm{A}}(t)}{R_0} + \delta f \left(\beta_{\mathrm{hot}}, \frac{\mathrm{d}^2 q}{\mathrm{d}r^2} \right) + \Delta f \tag{3}$$

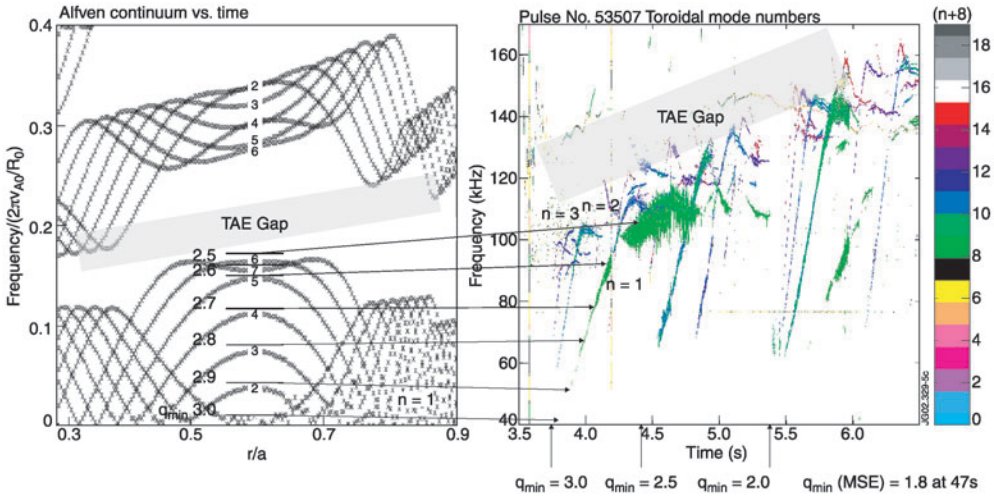

Figure 5. Correspondence between the evolution of the Alfvén continuum and the appearance of Alfvén Cascades of different toroidal mode numbers driven by ICRH ions in JET advanced scenarios with non-monotonic q-profile. The exact time of the crossing of the $q_{\min}$ rational values can be determined with great accuracy.

Here Δf is a fixed offset and δf is a small deviation of the cascade frequency from the Alfvén continuum, depending on the fast ion pressure and the second derivative of $q(r)$ at the point of zero magnetic shear. The finite value of δf allows ACs to avoid strong continuum damping.

Modes of different n satisfy the condition $m–nq_{\min} = 0$ at different times at which $q_{\min}$ passes different rational magnetic surfaces. Thus, the observation of the cascade frequencies provides information on $q_{\min}(t)$. For example, the $n = 1$ rational surfaces occur when $q_{\min}$ passes integer values $1, 2, 3\ldots$; the $n = 2$ rational surfaces occur when $q_{\min}$ passes integer and half-integer values $1, 3/2, 2, 5/2\ldots$, and so on.

Figure 5 illustrates this principle in a JET discharge with deeply reversed q-profile due to LH pre-heating. The Alfvén continuum structure for $n = 1$ is shown on the left for different times corresponding to the evolution of the value of $q_{\min}$. The curves labelled 1 through 8 on the figure are also identified by the values of $q_{\min}$ indicated on the plot, from 3 to 2.5. The arrows indicate the correlation with the observed $n = 1$ AC frequency evolution. At the point where the AC frequencies tend to cross their minimum value, for example around $t = 3.75$, we can infer that $q_{\min}$ passes an integer value. A single equilibrium reconstruction, performed including data from the motional Stark effect diagnostics for $t = 7$ s, is sufficient to determine which value of $q_{\min}$ is crossed at that time ($q_{\min} = 3$), as well as at the subsequent ones, as indicated. The accuracy with which the value of $q_{\min}$ is determined at a precise time is very high and provides a novel tool to investigate the dynamics of the creation of internal transport barriers (ITBs), as ITB triggering events are often associated with integer $q_{\min}$ surfaces.

3.3. Plasma mass determination from active AE measurements

The square root dependence on the plasma mass has suggested, since the early experiments on Alfvén waves in tokamaks, the diagnostic potential of the AE frequency measurements for determining the plasma isotopic mix [18]. Local measurements of Global AEs, existing just below a local minimum of the Alfvén continuum in the plasma core, were proposed [19]. After the discovery of new classes of AEs, including TAEs and EAEs, the same principle was

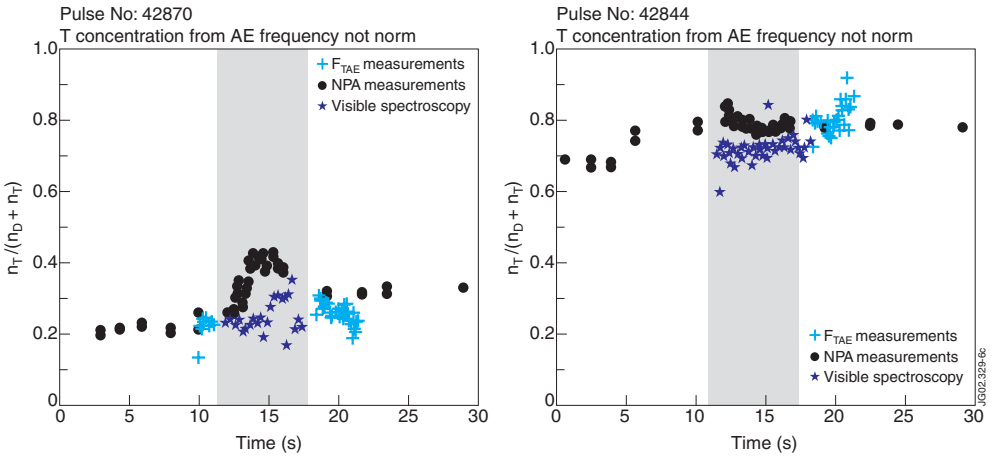

Figure 6. Estimate of D–T ratio from the measured frequency of an externally excited $n = 1$ TAE compared with visible spectroscopic data (intensity ratio of T_α to D_α lines) and with results from the neutral particle analyzer [5].

further investigated [20] and tested on the JET D–T plasmas. An example of the results is shown in figure 6, where the measurement of the plasma effective mass, i.e. the D/T ratio, is performed in a series of discharges with similar equilibrium characteristics [21]. In this case direct estimates can be obtained purely from experimental measurements. Focusing on relative changes of the ion mass, we can neglect the contribution from impurities and obtain [22]

$$\frac{n_\mathrm{T}}{n_\mathrm{D} + n_\mathrm{T}} = A_\mathrm{eff} - 2 \tag{4}$$

$$\frac{n_\mathrm{T}}{n_\mathrm{D} + n_\mathrm{T}} = 2\left[\left(\frac{f_\mathrm{TAE}^\mathrm{D-D} K(n)}{f_\mathrm{measured}}\right)^2 - 1\right] \tag{5}$$

f_TAE^{D-D} is calculated from the average density $\langle n_e \rangle$, $q = 1.5$ and $A_\mathrm{eff} = 2$; $K(n)$ is a calibration factor obtained from similar D–D shots, accounting for the difference between the actual density and q values at the TAE location, $n_\mathrm{e}(r_\mathrm{TAE})\, q(r_\mathrm{TAE})$, and $\langle n_\mathrm{e} \rangle$ and $q = 1.5$. Figure 6 suggests a good agreement with edge spectroscopic measurements for two discharges with different D/T relative concentrations, although with a somewhat different time evolution. This method may be useful in a reactor, where the same plasma configuration will repeatedly be employed. Direct measurements are possible in real time for similar equilibria, with a time resolution of the order of 30 ms, the time needed to scan across a resonance. Spatially, we can consider that the measurement is averaged over the global mode structure, encompassing the core region, to which conventional spectroscopic methods are not sensitive. The overall accuracy depends on the reproducibility of the equilibrium. When the equilibrium is significantly varied from shot to shot along with the isotopic mix, one must rely upon a full theoretical analysis, losing the real time capability.

The new multiple antenna system discussed above (see figure 3), which will be able to drive higher n harmonics, could enable us to perform tracking of individual resonances throughout plasma discharges, possibly including the divertor phase. The possibility of following more than one toroidal harmonic at a time will also be explored, to strengthen the constraint on the mass determination and correct for the Doppler shift due to plasma toroidal rotation in the high performance phase of the discharges.

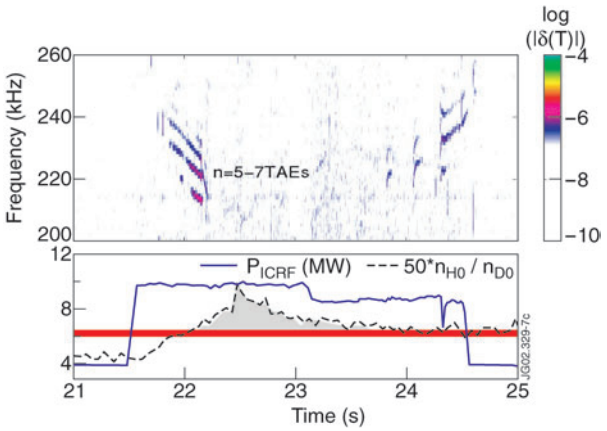

Figure 7. Suppression of the AE instability driven by ICRH power by the increase in the H minority concentration. This result shows that the AE stability limits can be used to infer in this case the tail ion energy content.

4. From AE stability to fast particle properties

As shown in equation (2), two conditions must be satisfied for AE instabilities to exist: fast particles must resonate in their motion with the phase velocity of the wave, and the free energy source for the instability, their radial pressure gradient, must be sufficiently strong. In this section we will illustrate examples of how the observation of unstable AEs can provide information on the fast ion energy content and their pressure gradient. The fast ions are produced by ICRH in JET conventional scenarios. In the case of H-minority heating in D plasmas, for a relative concentration of H of less than 10%, an ICRH power of 5 MW, corresponding to about 1 W cm^{-3}, produces a H^+ tail up to at least 0.5 MeV, as calculated by the PION code [23].

4.1. Fast particle energy tail

In addition to the ICRH power, a factor determining the creation of a tail in the H^+ distribution in D plasmas is the H/D relative concentration. For a given ICRH scenario, the AE stability limits therefore depend on this value. To illustrate this, we show in figure 7 a discharge in which the plasma equilibrium is maintained stationary, with a fully relaxed current profile. The ICRH power is kept above a level of 8 MW, but the H/D ratio is varied. The measured H/D ratio is shown at the bottom, while the top shows a detail of the magnetic spectrogram, corresponding to the TAE gap. When the H/D concentration ratio exceeds the value of about 13%, as measured at the plasma edge by optical spectroscopy, the ICRH-driven AE instabilities disappear, indicating that the ion tail does not reach resonant energies. Based purely on experimental observations, we can establish a link between H/D ratio and tail energy content; as the H/D ratio exceeds 13%, the number of fast ions with energies in the MeV range, resonating with the AEs, is significantly reduced. Such reduction is confirmed by data from a high-energy neutral particle analyser.

A second example comes from experiments in which third harmonic ICRH heating of He^4 in He^4 plasmas is used to create high-energy tails of α-particles, of interest for investigating the physics of burning plasmas in present devices [24]. The use of third harmonic is needed as the absorption at the fundamental would be too small, and at the second and the fourth harmonics

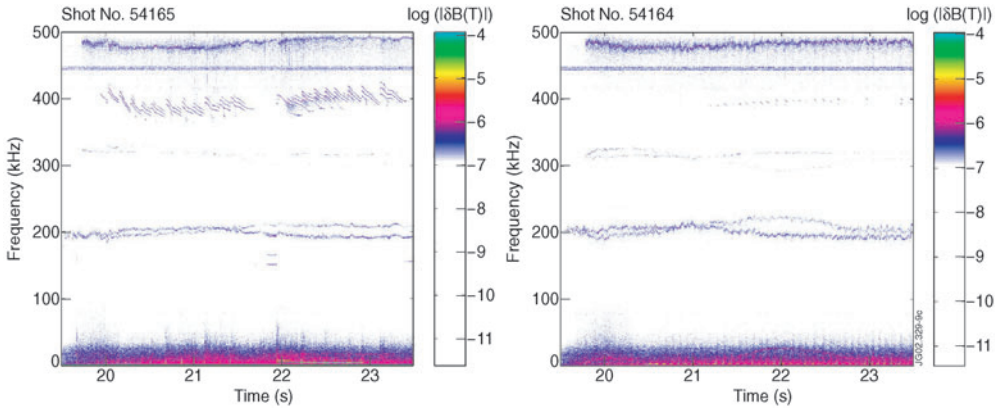

Figure 8. Comparison of magnetic spectrograms from two similar discharges with $f \approx 3 f_{ci}(^4\text{He})$ ICRH, one with 120 keV, relatively low density and $\rho_{beam} \sim 2.2$ cm (left), and the other with 70 keV beams, higher density and $\rho_{beam} \sim 1.4$ cm (right). Only the higher energy case shows TAE and EAE instabilities in the 150–200 kHz and 360–420 kHz ranges, signature of the production of α-tails in the MeV range [24].

would be too strongly affected by residual H-amounts in the vessel. As the absorption at $f = 3 f_{ci}$ is a finite Larmor radius effect, ions with a relatively large initial energy must be created by NBI injection. The measurements reported in figure 8 show that an important difference exist between NBI ions at 70 keV and at 120 keV. In the lower energy case the absorption is much weaker. Effects typically associated with fast particle tail in the plasma core, such as strong electron heating and stabilization of sawteeth, are observed only in the higher energy case. The measured unstable AEs shown in figure 8, the first α-driven AEs observed on JET, indicate that only in the case of 120 keV NBI α's reach energies in the MeV range. Note that, due to a larger value of the ratio v_A/v_{thi}, the ion Landau damping is reduced and AE collective effects are easier to observe than in equivalent D–T plasmas. In the neutron-free He^4 plasma, this result can be confirmed by γ-rays spectroscopy of threshold nuclear reaction $^9\text{Be}(\alpha, n\gamma)^{12}\text{C}$ [25], which suggests the presence of ^{4}He ions in the energy range 2 MeV. The scenario of third harmonic ICRH on He^4 plasma heated by 120 keV NBI is therefore suitable to produce significant α-particle tails in JET [24].

4.2. Fast particle pressure gradient

The possibility of obtaining information on the static fast particle pressure gradient has been illustrated in a number of past experiments on JET. It has been shown for example that due to the sign of the destabilizing term for AEs, appearing in equation (2), the presence of unstable negative mode numbers reveals the existence of a non-monotonic fast particle profile [26]. It has also been demonstrated experimentally that unstable AEs could be associated with a phasing of ICRH antennas that would produce an inward fast particle pinch, while no AEs were observed in the opposite case [27]. Here we show that such information can also be related to the dynamical evolution of the fast particle pressure gradient. We consider a case in which the current profile is monotonic and completely relaxed, with central q values just below unity, producing regular sawteeth events. TAEs and EAEs are driven unstable by 8 MW of ICRH power, with a H/D relative concentration of about 10%.

We note that at each saw-tooth crash, the TAE instability disappears for a short period of time (figure 9). This time interval is of the order of 100 ms, shorter than the slowing down time

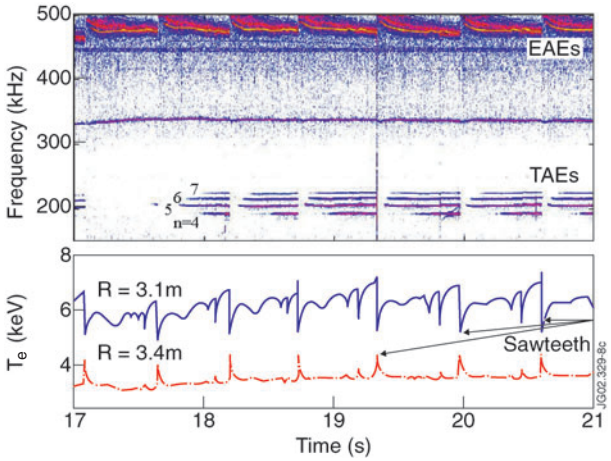

Figure 9. Effect of saw tooth crashes on the TAE and EAE stability in the presence of H-minority heating ICRH, with $P_{\mathrm{ICRH}} \sim 8$ MW, and H/D $\sim 10\%$.

for $\sim$0.5 MeV ions. It is therefore related to a rapid radial redistribution of fast ions associated with each saw tooth crash. The amplitude of the EAE instabilities is not affected significantly. This is due to the fact that for the equilibrium of the discharge under consideration, the TAE mode structure is core localized, peaking around $r/a \sim 0.3$, while the EAE peaks at a larger radial position, around $r/a \sim 0.45$, as reconstructed from the MISHKA MHD code [28]. Such an argument is supported by the fact that the Doppler shift of different toroidal harmonics, visible in the spectrogram, is larger for TAEs than for EAEs, corresponding to regions of strong and weak toroidal rotation, respectively. Note that the EAE frequency is affected by a sudden variation in the density and possibly in the local value of q [29].

4.3. Fast particle phase space local diffusion

A piece of information that the study of the AE spectrum can bring, which is inaccessible to any other diagnostic method, is the effective collision frequency in the phase space for particles resonating with the AEs [30]. This can be extracted from a detailed comparison of the AE spectra in the nonlinear phase of their evolution with the results of a general theory based on a model equation for the AE amplitude evolution $A(t)$ [31]:

$$\exp(-\mathrm{i}\phi)\frac{\mathrm{d}A}{\mathrm{d}t} = \frac{\gamma}{\cos\phi}A - \frac{\gamma_{\mathrm{L}}}{2}\int_0^{t/2}\tau^2\,\mathrm{d}\tau\int_0^{t-2\tau}\mathrm{d}\tau_1\exp\left[-\nu_{\mathrm{eff}}^3\tau^2\left(\frac{2\tau}{3}+\tau_1\right)\right] \times A(t-\tau)A(t-\tau-\tau_1)A^*(t-2\tau-\tau_1) \tag{6}$$

The amplitude evolution, and in particular the nonlinear regime that $A(t)$ falls into, is determined by a competition between the mode growth from the net drive (γ) and the replenishment of the distribution function in the region of the resonance with the mode. The latter mechanism is quantified by ν_{eff}, the effective collision frequency for the particles that resonate with the mode. All regimes predicted from equation (6) have been observed at JET for ICRH driven AEs in conventional and advanced scenarios of plasma operation [32, 33]. For the case of transition to a limit cycle behaviour, quantitative estimates of γ and ν_{eff} are obtained. Considering the example of a $n = 7$ TAE, we find that the value of γ ($\sim 8.5 \times 10^3\ \mathrm{s}^{-1}$) is in agreement with the expectations from the linear stability theory and with the direct measurements of damping and fast particle drive using active MHD spectroscopy.

The measured $\nu_{\rm eff}$ ($1.75 \times 10^4\ {\rm s}^{-1}$), on the other hand, is too large to be explained by classical collisions, and is suggestive of a direct effect of the ICRH power on the energetic particles. These estimates open the way to an evaluation of phase space transport for fusion-produced α's, important for plasmas on their way to ignition.

5. Conclusions and further developments

The investigation of the properties of collective modes in magnetized plasmas is used to extract information on the plasma from the measurement of the modes. Alfvén waves are the collective modes with the largest diagnostic potential both for the plasma bulk and the energetic particle population, as their frequency range is essentially free of incoherent fluctuations, waves can be exempt from strong damping, and non-perturbative, small amplitude modes can be detected.

Active and passive MHD spectroscopy, based on external antenna excitation and fast particle intrinsic drive, have been used to reveal a number of properties of the JET plasmas. Plasma bulk characteristics are extracted from the mode frequency. The examples discussed herein include equilibrium quantities, such as $q(r)$ in the plasma core and $n_{\rm e}(r)$ at the edge, and the fast evolution of the minimum value of the q-profile in advanced scenarios with non-monotonic q-profile. The plasma effective mass can also be extracted from the frequency of externally driven modes; for reproducible plasma equilibria, such information can be available in real time during a discharge. Information on fast ion energies and pressure gradients, including their dynamical evolution, can be obtained by observing the AE stability limits. The nonlinear development of AEs, if compared with fundamental nonlinear theory, can also provide information on the phase space dynamics of fast particles.

In principle, both active and passive spectroscopy can be employed in next step devices, such as ITER. The passive method of observing intrinsically unstable modes will benefit from the recent developments in fast data acquisition and storage and from the fact that in ITER or other plasmas with significant production of α's by fusion reaction, AEs of benign nature are expected to be present in most plasma conditions. The active method would necessitate an antenna structure able to drive low amplitude modes in the range 10–1000 kHz, perhaps making use of in-vessel components having a different main application, such as ICRH antennas. To test the possibility of driving intermediate toroidal mode numbers in the plasma core throughout plasma discharges using a small in-vessel structure, and the active MHD diagnostic potential for future experiments such as ITER, a new AE antenna for JET is being designed.

Use of MHD spectroscopy is not limited to fusion and laboratory plasmas. MHD waves are predicted to exist in a number of astrophysical plasmas, such as accretion disks [34] or coronal loops. For example, recent theoretical developments indicate that AEs induced by the density stratification along the loop can exist in coronal loops [35]. Remote observation of the properties of these modes could be used to extract information on the plasma local parameters.

Acknowledgments

This work was partly conducted under the European Fusion Development Agreement and some of the experiments were carried out within a JET-CRPP Task Agreement and within a JET-MIT collaboration supported by DoE Contract DE-FG02-99ER5-456.

References

[1] Goedbloed J P *et al* 1994 *Plasma Phys. Control. Fusion* **35** B277
[2] Cheng C Z, Chen L and Chance M S 1985 *Ann. Phys., NY* **161** 21

[3] Wong K L 1999 *Plasma Phys. Control. Fusion* **41** R1
[4] Heeter R F, Fasoli A, Ali-Arshad S and Moret J M 2000 *Rev. Sci. Instrum.* **71** 4092
[5] Fasoli A *et al* 1997 *Plasma Phys. Control. Fusion* **39** B287
[6] Fasoli A *et al* 1995 *Phys. Rev. Lett.* **75** 645
[7] Jaun A *et al* 2001 *Plasma Phys. Control. Fusion* **43** A207
[8] Testa D *et al* 2002 *Phys. Plasmas* **9** 243
[9] Fasoli A *et al* 1998 *Phys. Rev. Lett.* **81** 5564
[10] Huysmans G T A *et al* 1995 *Phys. Plasmas* **2** 1605
[11] Holties H, Fasoli A and Goedbloed J P 1997 *Phys. Plasmas* **4** 709
[12] Gormezano C *et al* 1998 *Phys. Rev. Lett.* **80** 5544
[13] Sharapov S *et al* 2001 *Phys. Lett.* A **289** 127
[14] Kimura H *et al* 1998 *Nucl. Fusion* **38** 1303
[15] Zonca F *et al* 2002 *PoP* submitted
[16] Berk H L *et al* 2001 *Phys. Rev. Lett.* **87** 185002
[17] Sharapov S *et al* 2002 *Phys. Plasmas* **9**
[18] Collins G A *et al* 1987 *Plasma Phys. Control. Fusion* **29** 323
[19] Descamps P *et al* 1990 *Phys. Lett.* A **143** 311
[20] Lister J B, Villard L and de Ridder G 1998 *Plasma Phys. Control. Fusion* **40** 1635
[21] Thomas P R *et al* 1998 *Phys. Rev. Lett.* **80** 5548
[22] Fasoli A *et al Phys. Plasmas* **7** 1816
[23] Eriksson L-G, Hellsten T and Willen U 1993 *Nucl. Fusion* **33** 1037
[24] Mantsinen M J *et al* 2002 *Phys. Rev. Lett.* **88** 105002
[25] Kiptily V G 1990 *Fusion Technol.* **18** 583
[26] Heeter R F 1999 *PhD Thesis* Princeton University
[27] Ericksson L *et al* 1998 *Phys. Rev. Lett.* **81** 1231
[28] Sharapov S *et al* 1999 *Nucl. Fusion* **39** 373
[29] Saigusa M *et al* 1998 *Plasma Phys. Control. Fusion* **40** 1647
[30] Heeter R F, Fasoli A, Sharapov S and Testa D 2002 *Phys. Plasmas* submitted
[31] Berk H, Breizman B N and Pekker M S 1997 *Plasma Phys. Rep.* **23** 778
[32] Fasoli A *et al* 1998 *Phys. Rev. Lett.* **81** 5564
[33] Heeter R F, Fasoli A and Sharapov S 2000 *Phys. Rev. Lett.* **85** 3177
[34] Keppens R, Casse F and Goedbloed J P 2002 *Astrophys. J. Lett.* **569** L121
[35] Beliën A J C, Poedts S and Goedbloed J P 1996 *Phys. Rev. Lett.* **76** 567